J. Membrane Biol. 134, 15–29 (1993)

The Journal of
Membrane
Biology

Deposition of $BaSO_4$ in the Tight Junctions of Amphibian Epithelia Causes their Opening; Apical Ca^{2+} Reverses this Effect

Jorge A. Castro[1], Antonio Sesso[2], F. Lacaz-Vieira[3]

[1]Departamento de Ciências Fisiológicas, Universidade do Rio Grande, Rio Grande, RS, Brasil
[2]Departamento de Patologia, Laboratório de Patologia Molecular, Faculdade de Medicina, Universidade de São Paulo, São Paulo, SP, Brasil
[3]Departamento de Fisiologia e Biofísica, Instituto de Ciências Biomédicas, Universidade de São Paulo, São Paulo, 05508-900, SP, Brasil

Received: 2 June 1992/Revised: 1 December 1992

Abstract. Selective deposition of $BaSO_4$ in the tight junctions (TJs) of frog skins led to profound and reversible functional alterations of these structures, as revealed by changes of tissue conductance (G), clamping current (I), and fluxes of extracellular markers (sulfate (J^{SO_4}) and sucrose (J^{SUC})). Experiments were performed with nominally Ca^{2+}-free simple salt solutions on the apical side (usually KCl) and Na_2SO_4-Ringer on the inner side of skins. The deposition of $BaSO_4$ in the TJs was obtained by diffusion and/or migration through the paracellular path of Ba^{2+} from the apical solution and SO_4^{2-} from the inner solution. A brief presence (2 to 6 min) of apical Ba^{2+} (Ba^{2+} pulse) is followed (i.e., when Ba^{2+} is removed from the apical fluid) by a large increase of G, I, J^{SO_4} and J^{SUC}, above pre-Ba^{2+} levels. These attain a steady state within 15 to 30 min (overshoot phase), characterizing a conspicuous increase of the paracellular permeability. During the overshoot phase, a second Ba^{2+} pulse blocks the paracellular route while apical Ba^{2+} is present, leading to a new and larger overshoot when the Ba^{2+} pulse is terminated. Addition of apical Ca^{2+} triggers the resealing of the TJs, resulting in a full recovery of G, I, J^{SO_4} and J^{SUC}. This Ca^{2+}-induced recovery persists when apical Ca^{2+} is removed. The presence of a normal Ca^{2+} concentration in the inner bathing Ringer does not induce the recovery process. Tissues remain viable after being submitted to the Ba^{2+} treatment and the subsequent overshoot. Experiments performed in the urinary bladder of *Rana catesbeiana* and skins and urinary bladders of *Bufo marinus* indicate that Ba^{2+} effect can also be elicited in these tissues. The above results seem to report general properties of the TJs. Incidentally, they warn about the use of Ba^{2+} as an ion channel blocker in epithelial membranes in association with SO_4^{2-}-containing solutions on the contralateral side.

Key words: Amphibian skin—Amphibian urinary bladder—Tight junction—Paracellular path—Calcium—Barium

Introduction

The *zonula occludens* (ZO), originally described in amphibian skins (Farquhar & Palade, 1965), is the outermost part of the junctional complex of epithelial membranes. It is constituted by a tight junction (TJ) that completely circumscribes the apex of the epithelial cells. Two major functions are currently attributed to the ZO: (i) control of the permeability of the paracellular pathway, and (ii) polarization of the epithelial cells, separating two functionally distinct regions, the apical and basolateral membrane domains (Erlij & Martínez-Palomo, 1978; Simons & Fuller, 1985; Cereijido et al., 1988; Cereijido, Contreras & González-Mariscal, 1989*a*; Cereijido, Ponce & González-Mariscal, 1989*b*; Simons, 1990).

Although the ZO has been well characterized from the functional point of view, little is known about its molecular composition (Gumbiner, 1987; Simons, 1990). Several polypeptides have been found in close association with TJs of several epithelia (Griepp et al., 1983; Gumbiner & Simons, 1986;

Correspondence to: F. Lacaz-Vieira

Stevenson et al., 1986; Citi et al., 1988). Junction formation is apparently controlled by a network of reactions where G proteins, phospholipase C, adenylate cyclase, protein kinase C, and calmodulin might be involved (Balda et al., 1991).

The knowledge of the supramolecular organization of the ZO is mostly based on ultrastructural findings (thin-section and freeze-fracture electron microscopy). In freeze-fracture electron microscopy the ZO appears as a network of intramembrane strands which bring the plasma membranes into close apposition (Chalcroft & Bullivant, 1970; Goodenough & Revel, 1970; Wade & Karnovsky, 1974; Hirokawa, 1982; Kachar & Reese, 1982; Pinto da Silva & Kachar, 1982; Stevenson & Goodenough, 1984). These strands correspond to contacts observed in thin sections and might be constituted by a row of protein molecules, or of pairs of inverted cylindrical micelles sandwiched between linear fusions of the external membrane leaflets of adjacent cells (*for review see* Kachar & Reese, 1982; Gumbiner, 1987; Cereijido et al., 1989*b*; Simons, 1990). Microfilaments apparently play a role in positioning junctional strands, influencing the sealing of TJs (Meza et al., 1980).

The electrical resistance of the paracellular pathway is mainly determined by the ZO. The degree of tightness of the ZO has been correlated to the number of junctional strands lying parallel to the surface of the epithelium (Claude & Goodenough, 1973; Claude, 1978; Easter, Wade & Boyer, 1983; Marcial, Carlson & Madara, 1984; Madara & Dharmsathaphorn, 1985), although exceptions have been suggested (Martínez-Palomo & Erlij, 1975; Mazariegos, Tice & Hand, 1984). According to the permeability of the ZO, epithelial membranes can be ranked from "leaky epithelia," with resistance in the order of 5 Ω cm^2 (such as renal proximal tubule), to "extremely tight epithelia" (such as the urinary bladder of amphibia), with several thousand Ω cm^2. Amphibian skins are moderately tight epithelia (Ussing, Erlij & Lassen, 1974; Erlij & Martínez-Palomo, 1978).

Different procedures have been shown to affect the permeability of the ZO in natural epithelia as well as in cultured monolayers. Permeability increases were shown to result from: apical hypertonicity (Ussing & Windhager, 1964; Erlij & Martínez-Palomo, 1972; Wade, Revel & Discala, 1973; González et al., 1978), chelation of extracellular Ca^{2+} (Sedar & Forte, 1964; Cereijido et al., 1978; Meldolesi et al., 1978; Pitelka, Taggart & Hamamoto, 1983) low pH in the apical solution (Fischbarg & Whittembury, 1978; González et al., 1978; Benedictis & Lacaz-Vieira, 1982), rise of cell Ca^{2+} concentration (Cereijido, Meza & Martínez-Palomo, 1981), accumulation of Li^+ within the cell (Aboulafia, Sanioto & Lacaz-Vieira, 1983), among others (*see* Cereijido et al., 1988). In addition, various agents have been reported to reduce the permeability of the paracellular pathway. They include 2,4,6-triaminopyrimidine (Moreno, 1974, 1975; Reuss & Grady, 1979), plant cytokinins (Bentzel et al., 1976; Bentzel et al., 1980) and protamine (Bentzel et al., 1987). In *Necturus* gallbladder, Ba^{2+} increases the resistance of the paracellular pathway through an unknown mechanism (Kottra & Fromter, 1990), in addition to blocking apical and basolateral K^+ channels.

The aim of the present work was to study the effects of a selective deposition of $BaSO_4$ in the paracellular pathway on the permeability of the TJs, the main barrier in this route. The real stimulus to this work came when we observed during studies of Ba^{2+} effect on apical cation channels (with SO_4^{2-} as the major anion on the inner side), that removal of Ba^{2+} from the apical solution caused an unexpectedly large increase of transepithelial conductance.

No similar result seems to have been reported up to now, although the exposure of the apical surface of amphibian epithelia to Ba^{2+} has been accomplished in a wide variety of experimental circumstances as a procedure for blocking ion channels (Ramsay et al., 1976; Van Driessche & Zeiske, 1980, 1985; Granitzer & Nagel, 1990; Van Driessche & De Wolf, 1991), or marking the intercellular space with $BaSO_4$ for electron microscopy (Ussing, 1971; Wade et al., 1973).

Materials and Methods

Preparation

Abdominal skins of double pithed bullfrog *R. catesbeiana* were used in most of the experiments. Additional experiments were carried out in urinary bladders of the same species and in skins and bladders of *B. marinus*. Special mention to the kind of preparation used will be made in these cases. Otherwise, the results were obtained in skins of *R. catesbeiana*. Tissue fragments glued to plastic rings (De Wolf & Van Driessche, 1986) of 20 mm diameter with ethylcyanoacrylate adhesive (Super Bonder, Loctite Brasil) were mounted in a modified Ussing chamber, exposing an area of 0.5 cm^2. Tissue-edge damage was avoided by using hemichambers with a recessed rim filled with a high viscosity silicone grease (Silicon DC high vacuum grease, Riedel, De Haen AG) (Lacaz-Vieira, 1986). Each chamber compartment was perfused with a continuous flow of solution (up to 25 ml/min), driven by gravity from reservoirs through plastic tubings. The formation of a layer of stagnant fluid adjacent to the tissue was prevented by directing the incoming fluid towards its surface. The fluid left each compartment through a spillway open to atmosphere, so that the pressure in both compartments was kept near atmospheric. Rapid solution changes were obtained without interruption of voltage clamping

by switching the plastic tubings at their connections with the chamber.

Electrical Measurements

A conventional voltage clamp (Yale University, Department of Physiology) with continuous feedback was used. Saturated calomel half-cells with 3 M KCl agar bridges were used to measure the electrical potential difference across the skin. Current was passed through Ag-AgCl 3 M KCl electrodes and 3 M KCl agar bridges, adequately placed to deliver a uniform current density across the skin. The clamping current was continuously recorded by a strip-chart recorder.

Isotopic Flux Measurements

The labeled compound was added to the inner solution which was recirculated with a peristaltic pump at a rate of 5 ml/min. An equilibration period of at least 20 min following isotope addition, during which the apical solution was continuously renewed, was allowed before sampling of the apical solution. During the collection period, the flow of solution through the apical compartment was stopped, while the apical solution was kept vigorously stirred by a plastic propeller driven by an electric motor. At the end of the collection interval, the solution was sampled for radioactivity assay. Subsequently, solution was again allowed to flow through the apical compartment until the next collection period. Carrier-free Na_2SO_4 labeled with ^{35}S was obtained from Instituto de Pesquisas Energéticas e Nucleares (São Paulo), and ^{14}C-sucrose, from Amersham Laboratories (England).

Electron Microscopy

Skins or bladders were removed from the chamber and, while still glued to the plastic ring, were immersed for a few minutes in 2% glutaraldehyde buffered with 0.1 M phosphate. From the central area a small tissue fragment was punched out and kept in the same fixative solution from 24 to 48 hr before further processing. The fragments were then treated for one hour with 1% osmium tetroxide, dehydrated in series of ethanol saturated with $BaSO_4$, immersed in propilene oxide and embedded in Araldite. The sections were collected in 10 mM $BaCl_2$ saturated with $BaSO_4$. Solutions were saturated with $BaSO_4$ to prevent dissolution of the $BaSO_4$ likely formed in the tissue (Wade et al., 1973). Appropriate controls demonstrated that this procedure did not induce precipitate in control specimens. Sections were stained in 0.5% uranyl acetate in water and, later in lead citrate (Reynolds, 1963). Some specimens were not submitted to the last staining step. Sections were picked up on Formvar-coated supporting grids with parallel bars to expose maximum length of the epithelium, and examined in a Philips EM 301 electron microscope at 60 kV. Micrographs were taken at an electron optical magnification of 5,000–13,000× on 35 mm films.

Free Ca^{2+} Concentration

The free Ca^{2+} concentration in the bathing solutions was measured according to the following procedures: (i) in the nominally Ca^{2+}-free apical solutions, by the Fura-2 fluorescence method (Grynkiewicz, Poenie & Tsien, 1985), and (ii) in the solutions with added Ca^{2+}, with a Ca^{2+} ion electrode (Orion Research, model 93-20).

Solutions

The compositions of the solutions used on the inner side were (in mM): Na_2SO_4-Ringer: Na_2SO_4 57.5, $KHCO_3$ 2.5, and $CaSO_4$ 1.0 (free Ca^{2+} concentration 0.35 mM). NaCl-Ringer: NaCl 115, $KHCO_3$ 2.5, and $CaCl_2$ 1.0 (free Ca^{2+} concentration 1.0 mM). $NaNO_3$-Ringer was obtained replacing NO_3^- for Cl^- in the NaCl-Ringer. All the Ringer solutions had a pH of 8.2 after aeration. The apical bathing fluids were simple salt solutions, nonbuffered, without added Ca^{2+} (unless where specially stated), prepared with glass distilled water, having pH around 6.0 and a free Ca^{2+} concentration in the range of 1.5×10^{-7} and 2.0×10^{-7} M.

Experimental Protocols

Except when stated otherwise, the experiments were performed with Na_2SO_4-Ringer solution bathing the inner surface of skins or bladders.

Protocol 1

Tissues were voltage clamped at 40 mV with a KCl solution of 75 mM (or other specified value) on the apical surface. A pulse of Ba^{2+} was applied by adding 10 mM of $BaCl_2$ (or less, as specified) to the apical solution for a period of 4 min. Other times were also tested. The Ba^{2+} pulse was terminated by replacing the apical fluid by a fresh KCl solution of the same previous concentration.

Protocol 2

Tissues were short-circuited with a KCl solution of 75 mM on the apical surface. Isolated pulses of Ba^{2+} (6 min) or urea (2 min) on the apical surface were applied by replacing the apical solution by the same solution containing $BaCl_2$ 10 mM or urea 200 mM. The superposition of a pulse of urea on top of a Ba^{2+} pulse was obtained by replacing the Ba^{2+}-containing solution, 2 min after its addition to the apical compartment, with a solution containing Ba^{2+} and urea in the same concentrations as before. The pulses were terminated by replacing the apical solution with a fresh solution as in the beginning of the experiment.

Statistics

The results are presented as mean ± SEM. Comparisons were carried out using Student's paired *t*-test. When more than two groups were compared, significance was determined by two-way analysis of variance followed by appropriate post-test comparison. The *P* values cited include Bonferroni's correction (Neter & Wasserman, 1974).

Abbreviations and Conventions

G: Total transmembrane electrical conductance, in mS/cm^2. Calculated from the deflections of the clamping current induced by shifts of the clamping potential of 300 msec duration, ±5 mV

amplitude at 15 sec intervals, as $G = \Delta I/\Delta V$, where ΔV and ΔI are the changes in the electrical potential difference across the tissue and clamping current, respectively.

I: Clamping-current, in $\mu A/cm^2$. Positive current corresponds to the transport of positive charges across the tissue, from the apical to the inner bathing solution.

V: Electrical potential difference across the tissue, in mV. The potential of the apical solution is referred to that of the inner solution.

J: Fluxes, measured isotopically from internal to apical side, in $\mu A/cm^2$ for SO_4^{2-} (J^{SO_4}) or in pmol cm^{-2} min^{-1} for sucrose (J^{SUC}).

Results

1. Tissue Electrical Conductance Increases Markedly Following the End of a Brief Pulse of Ba^{2+} in the Apical Solution

These experiments aimed at inducing a selective deposition of $BaSO_4$ in the paracellular pathways and were carried out according to Protocol 1 (*see* Materials and Methods). K^+ was used as the main cation in the apical solution to rule out any contribution of apical Na^+ to the overall values of *G* and *I* (experiments with apical Na^+ are described in section 9 below). Cl^- was the major anion in the apical compartment so Ba^{2+} could be added to the apical solution without precipitation. The brief exposure of the apical skin surface to Ba^{2+} is called, for short. "Ba^{2+} pulse."

Figure 1*A* is a representative experiment showing that *G* declines slightly during the Ba^{2+} pulse and increases markedly, above control levels, when the pulse terminates, attaining steady-state values within 15 to 30 min. This increase of *G* above control levels in response to apical Ba^{2+} withdrawal, will be called "overshoot," for short. If the experimental conditions are maintained, the high conductance state that characterizes the overshoot remains stable for at least 1 hr (the largest time systematically studied). The clamping current (*I*) closely follows the time course of *G* (Fig. 1*A*). Mean values of *G* and *I* for a group of 25 skins are shown in Fig. 2*A* and *B*, respectively.

Readmission of Ba^{2+} to the apical solution during the overshoot phase causes a much larger drop of *G* and *I* (Fig. 1*A* and Table 1), than when Ba^{2+} was tested for the first time. When this second Ba^{2+} pulse is terminated, a new overshoot of higher size takes place (Figs. 1*A* and 9).

Some variations of Protocol 1 were tested: (i) the apical KCl concentration ranged between 50 and 100 mM; (ii) the apical Ba^{2+} varied between 2 and 10 mM; and (iii) the length of the Ba^{2+} pulse was between 2 and 6 min. As a rule, overshoots are larger

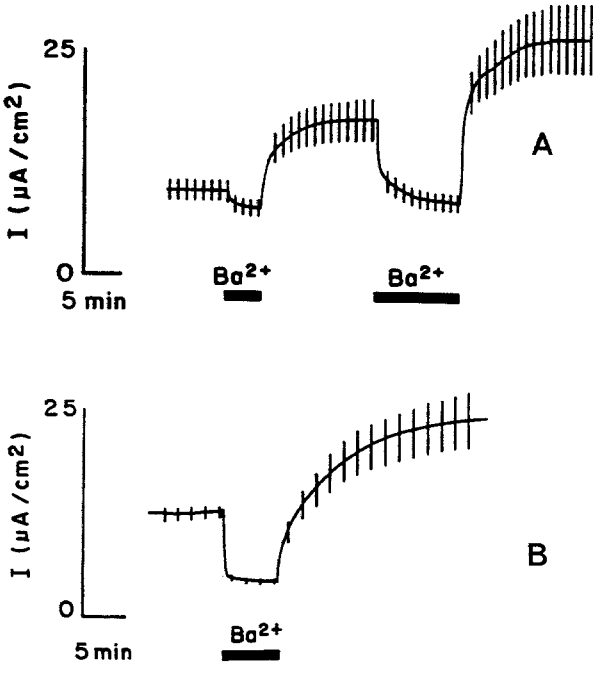

Fig. 1. Representative experiments performed in a frog skin (*A*) and in a frog urinary bladder (*B*), showing the time course of the clamping current (*I*) and conductance (*G*). *G* is proportional to the vertical deflections of *I*. Tissues were submitted to a Ba^{2+} pulse according to Protocol 1 (*see* Materials and Methods). Overshoots of *I* and *G* follow the end of the apical Ba^{2+} pulse. In *A*, the effect of a second Ba^{2+} pulse can also be observed.

when obtained with larger concentrations of apical KCl and larger pulses of Ba^{2+} (concentration and/or duration). However, for the general purpose of characterizing the response to Ba^{2+}, results obtained under those conditions are equivalent, since, in all cases, termination of the Ba^{2+} pulse is always followed by conspicuous increases of *G* and *I* above control levels.

Other tissues (urinary bladders of *R. catesbeiana* and skins and urinary bladders of *B. marinus*) were also tested following Protocol 1, and showed similar responses. Figure 1*B* shows a representative experiment in the urinary bladder of *R. catesbeiana*.

2. Selective Deposition of $BaSO_4$ in the TJs Leads to Functional Alterations of These Structures

As a result of several experimental conditions tested, it can be concluded that two requisites are essential to induce the overshoot phase: (i) Preexposure of the apical skin surface to Ba^{2+} ions. Pulses of Ca^{2+} or Mg^{2+} instead of Ba^{2+} failed to cause overshoot. (ii) A SO_4^{2-}-Ringer solution bath-

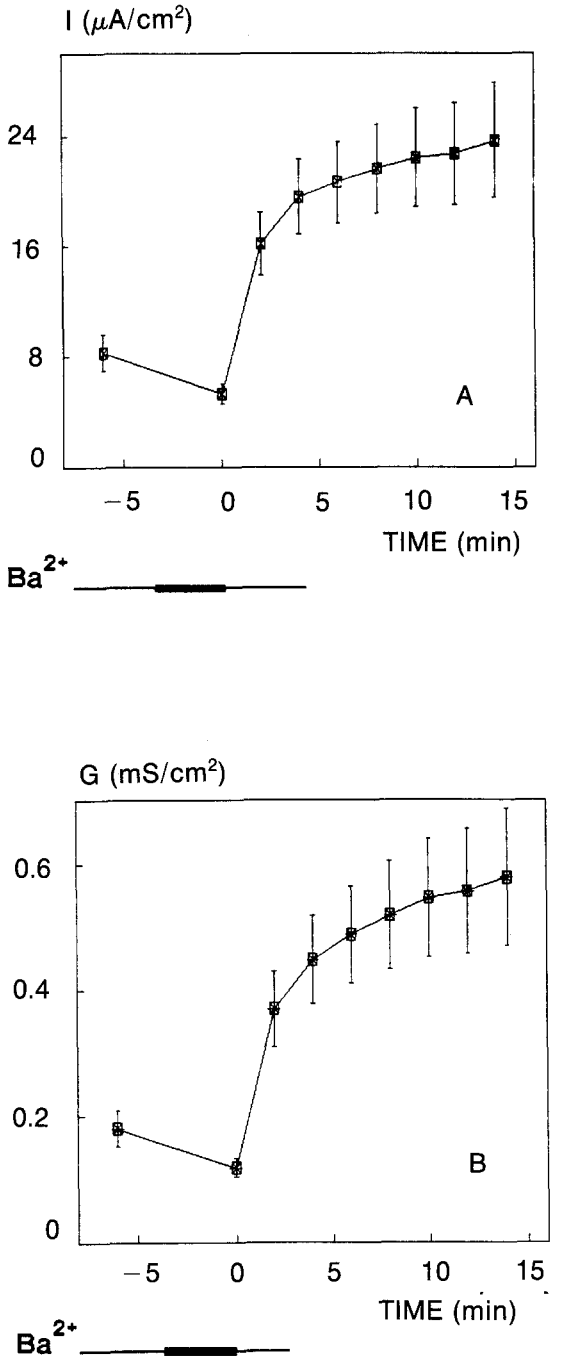

Fig. 2. Average values of the clamping current *I* (*A*) and conductance *G* (*B*) obtained in 25 frog skins submitted to an apical Ba^{2+} pulse according to Protocol 1 (*see* Materials and Methods). Time zero was set at the end of the Ba^{2+} pulse.

ing the inner skin surface. No effect was obtained with internal NaCl- (three skins) or $NaNO_3$-Ringer (three skins). A positive clamping potential (used in Protocol 1) helps induce the Ba^{2+} effect, but is not essential. As shown in Fig. 3, for a representative experiment of a group of six skins, a smaller overshoot was indeed induced by a Ba^{2+} pulse under the short-circuited condition, while a similar Ba^{2+} pulse applied under a negative clamping potential (−40 mV) failed to induce an overshoot. It can be inferred from these experiments that migration and/or diffusion of SO_4^{2-} from the inner solution and Ba^{2+} from the apical solution towards each other are somehow required for the overshoot to occur when the Ba^{2+} pulse is terminated. As the permeabilities of cell membranes to Ba^{2+} and SO_4^{2-} are rather low, a reasonable working hypothesis to start with would be that these ions interact within the paracellular pathway, leading to deposition of $BaSO_4$ in this region. This assumption is strengthened by the results of three experiments in which both the clamping polarity and the relative positions of Ba^{2+} and SO_4^{2-} ions in the bathing solutions were inverted. NaCl-Ringer solution with 10 mM $BaCl_2$ bathed the inner side of skins throughout the experiment. NaCl-Ringer replaced the Na_2SO_4-Ringer used in the usual experiments so Ba^{2+} could be introduced in the inner compartment. On the apical side, the skins were bathed by 100 mM KCl. A "sulfate pulse" (instead of a Ba^{2+} pulse) was applied by replacing the apical solution by a solution of 50 mM K_2SO_4 during 4 min under a negative clamping potential (−40 mV). Overshoots followed the end of the sulfate pulse. These overshoots were, however, smaller and slower compared to those described previously. No overshoot could be elicited in response to a sulfate pulse applied under 40 mV clamping potential.

3. The Opening of TJs by Urea Helps the Interaction of Ba^{2+} and SO_4^{2-} at the TJ Level

As shown by conductance and permeability increases and ultrastructural modifications, addition of urea to the apical solution, making it hypertonic to the internal Ringer solution, is a known procedure to open the TJs in tight epithelial membranes (Ussing & Windhager, 1964; Erlij & Martínez-Palomo, 1972; Wade et al., 1973; González et al., 1978). This feature of apical hypertonicity was used to examine whether the opening of the TJs by urea could, in the short-circuited condition, facilitate the interaction of Ba^{2+} and SO_4^{2-} in the paracellular pathway. In the short-circuited condition the overshoots are rather trifling, as already shown in Fig. 3.

The experiments were carried out in the short-circuited condition (Protocol 2). A representative

Table 1. Effect of apical Ba^{2+} on the clamping current (I) and conductance (G)

Experimental condition	Apical solution					
	KCl	KCl + Ba^{2+}		KCl	KCl + Ba^{2+}	
	I	I $\mu A/cm^2$	ΔI	G	G mS/cm^2	ΔG
Control	6.31 ± 0.92	4.77 ± 0.67	1.54 ± 0.36	0.18 ± 0.03	0.12 ± 0.01	0.06 ± 0.01
Overshoot	14.46 ± 1.67	5.09 ± 0.65	9.38 ± 1.30*	0.40 ± 0.04	0.14 ± 0.01	0.26 ± 0.03*

Average values obtained in 10 frog skins. Overshoots were induced according to Protocol 1 (*see* Materials and Methods). ΔI and ΔG are, respectively, the differences between I and G values measured in the absence and presence of apical Ba^{2+}, both in the control and in the overshoot phase. Statistical comparisons: (*) different from value in the control condition ($P < 0.001$), paired t-test.

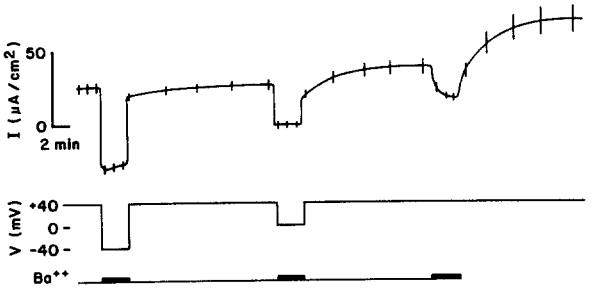

Fig. 3. Representative experiment in a frog skin showing the effect of Ba^{2+} pulses (10 mM $BaCl_2$ added to the apical solution for 4 min) upon the clamping current (I) and conductance (G) for three different values of the clamping potential (V): 40, 0 and −40 mV, during the pulse. The apical solution was 75 mM KCl. G is proportional to the vertical deflections of I.

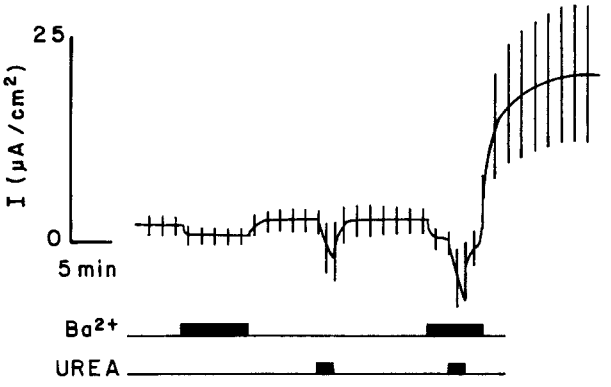

Fig. 4. Representative experiment in a frog skin showing the effect of the superimposition of a short pulse of urea on the Ba^{2+} pulse. The skin was short-circuited with 75 mM KCl as apical solution. I is the clamping current and the conductance G is proportional to the vertical deflections of I. Single pulses of Ba^{2+} (10 mM $BaCl_2$ added for 6 min to the apical solution) or urea (200 mM added for 2 min to the apical solution) cause only transient effects that revert almost entirely when the pulses are terminated. In contrast, when a pulse of urea (2 min, 200 mM) is superimposed on the pulse of Ba^{2+} (6 min, 10 mM), an overshoot is elicited.

experiment of a group of four skins is shown in Fig. 4. An isolated Ba^{2+} pulse causes a very small overshoot. A subsequent isolated pulse of urea increases the conductance, as expected (Ussing & Windhager, 1964; Erlij & Martínez-Palomo, 1972; Wade et al., 1973; González et al., 1978), and the effect is entirely reversible upon urea removal. Finally, a large overshoot results from a pulse of urea superimposed to a pulse of Ba^{2+}. As apical urea specifically acts at the TJ level (Ussing & Winhager, 1964; Erlij & Martínez-Palomo, 1972; Wade et al., 1973; González et al., 1978), the overshoot enhancement caused by a pulse of urea on top of a pulse of Ba^{2+} is a strong indication that the TJ is a limiting barrier for the migration of Ba^{2+} and SO_4^{2-} and that the interaction of these ions occurs at the TJ level during the Ba^{2+} pulse. Furthermore, the results discard any essential contribution *per se* of the reversed skin potential (apical solution positive), used in Protocol 1, to the genesis of the overshoot, as the skins were short-circuited throughout the experiment. This control is relevant, as skin depolarization has been claimed to open the shunt pathway in frog skins (Mandel & Curran, 1972).

The superimposition of pulses of urea and Ba^{2+} turned out to be a useful procedure (Protocol 2) for inducing overshoots without having to count on reversing the skin potential.

4. An Electron-Dense Material Can Be Found in the Intercellular Spaces at the End of a Ba^{2+} Pulse

To test the working hypothesis raised in section 2 above (formation of $BaSO_4$ in the intercellular

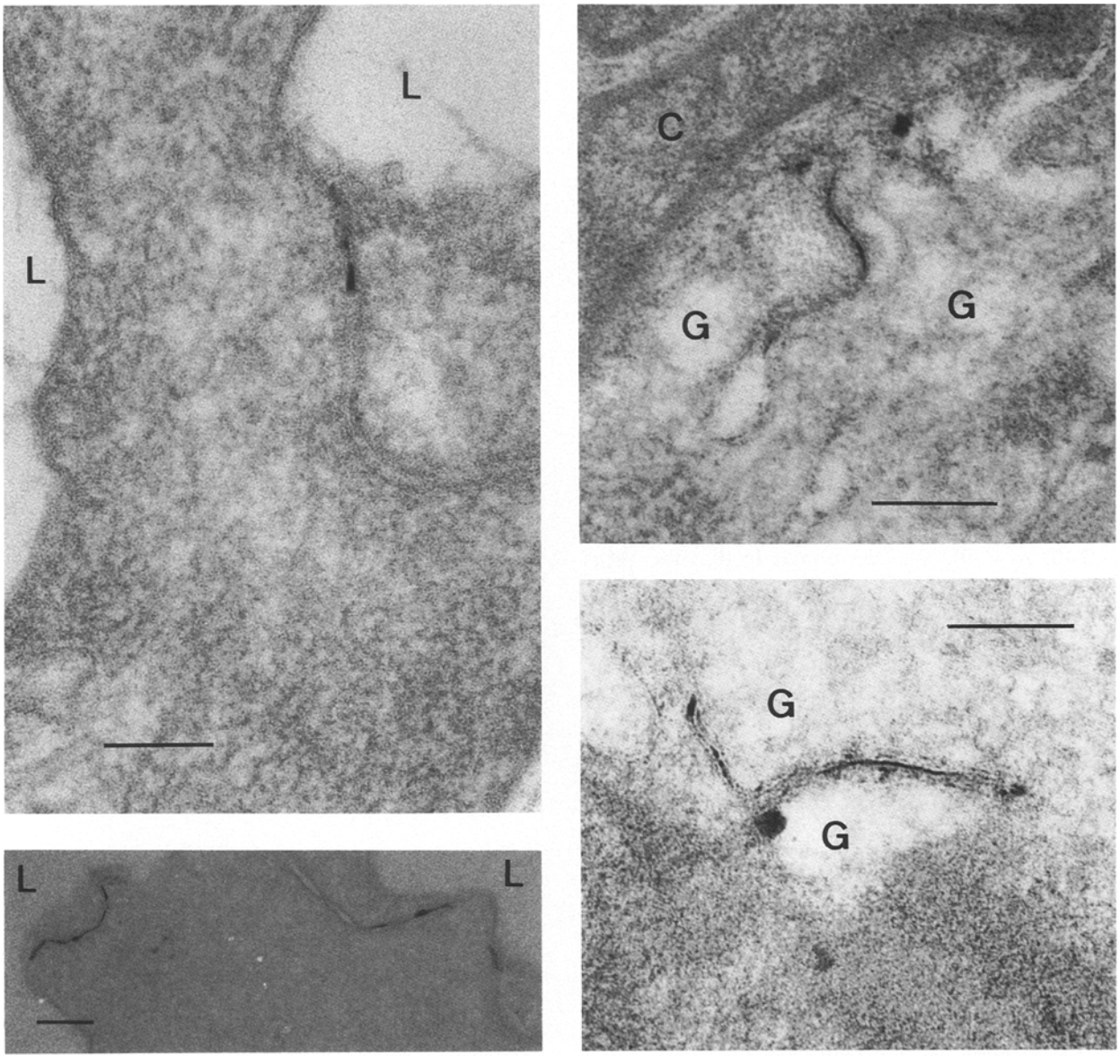

Fig. 5. Thin-section electron micrographs of frog urinary bladders and a frog skin fixed at the end of a Ba^{2+} pulse applied according to Protocol 1 (*see* Materials and Methods). **Left panel:** an electron-dense material is seen in two representative sections through the apical region of adjacent epithelial cells of urinary bladder. Staining by lead citrate was omitted in the specimen in the lower micrograph. *L* is the lumen of the bladder. **Right panel:** Two sections of frog skins showing regions just beneath the *stratum corneum* (*C*) where an electron-dense material is seen between plasma membranes of granular cells (*G*). Bars represent 0.1 μm.

spaces at the level of the TJs), transmission electron microscopy of thin sections was carried out. An electron-dense material (most certainly $BaSO_4$) was detected in skins and bladders fixed at the end of a Ba^{2+} pulse applied according to Protocol 1. This material was found in the intercellular spaces at the level where the ZOs are expected to occur, as shown in Fig. 5. Aside from the electron-dense material, the epithelia could not be distinguished from that of control skins or bladders not submitted to the Ba^{2+} treatment.

Skins or bladders fixed in the overshoot phase were virtually indistinguishable from controls not submitted to the Ba^{2+} treatment. Occasionally, fine remnants of the electron-dense material could be found in the intercellular spaces.

5. Skins Remain Viable after the Ba^{2+} Treatment

Experiments were performed to assess whether tissues remain viable after being submitted to the Ba^{2+} treatment and the resulting overshoot. For that purpose, the skin ability to perform active Na^+ transport was evaluated by the short-circuit current. The skins were initially short-circuited with Na_2SO_4-Ringer on both sides. When the short-circuit current was stable, the apical solution was replaced by 75 mM KCl and an overshoot induced according to Protocol 1. After the overshoot phase had evolved for 15 min, the skins were again short-circuited with Na_2SO_4-Ringer on the apical side. The short-circuit current stabilized, and its value one hour later (29.6 ± 5.8 $\mu A/cm^2$) was not significantly different from that observed at the end of the stabilization period in the beginning of the experiments (26.6 ± 4.4 $\mu A/cm^2$) ($P > 0.40$, $n = 9$). We can conclude that the skins remain viable after being submitted to a Ba^{2+} pulse and the subsequent period of conductance increase.

6. Apical Ca^{2+} Promotes the Resealing of TJs Opened during the Overshoot Phase

The following experiments show that (i) the conductance which is high in the overshoot phase fully recovers when Ca^{2+} is added to the apical solution, and (ii) recover is not triggered by the sole presence of Ca^{2+} in the basolateral solution.

As in all previous experiments, the overshoots were induced with a nominally Ca^{2+}-free apical KCl solution in which the free Ca^{2+} concentration was in the range of 1.5×10^{-7} to 2.0×10^{-7} M (*see* Materials and Methods).

Independent experiments performed in three skins ascertained that in the control condition (before the Ba^{2+} pulse) G and I are not affected by the apical Ca^{2+} concentration in the range of 10^{-7} M to 5 mM.

Two experimental groups were conducted to evaluate the recovery of conductance induced by addition of apical Ca^{2+}. *Group 1*—Overshoots were induced according to Protocol 1. Figure 6*A* shows a representative experiment and Fig. 7*A* mean values of G for 13 similar experiments. The protocol that was followed to induce recovery by apical Ca^{2+} is described in the legend of Fig. 6*A*. *Group 2*—Overshoots were induced according to Protocol 2. Figure 6*B* shows a representative experiment and Fig. 7*B* mean values of G for six similar experiments. The protocol that was followed to induce recovery by apical Ca^{2+} is described in the legend of Fig. 6*B*. The free Ca^{2+} concentration in the apical solution during the recovery phase of these experiments was adjusted to a value slightly lower (0.25 mM) than that in the Na_2SO_4-Ringer present on the inner compartment (0.35 mM). This aimed to rule out any increase of the free Ca^{2+} concentration in the interspaces by Ca^{2+} leaking through the TJs from the apical solution. Therefore, an indirect action of apical Ca^{2+} on the basolateral aspect of the cells could be discarded.

The main features of tissue response to the addition of Ca^{2+} to the apical solution are shared by the two groups, as exemplified in Fig. 6: (i) soon after Ca^{2+} is added to the apical solution G increases while I drops sharply, (ii) thereafter, G declines slowly and reaches eventually a value that is not significantly different from the control pre-Ba^{2+} level (Fig. 7), (iii) apical Ca^{2+} removal at the end of the recovery phase does not revert the Ca^{2+}-induced recovery. G values measured 15 min after Ca^{2+} removal are not significantly different from the value at the end of the recovery phase. Skins fully recovered behave as fresh tissues being able to withstand a new overshoot if a pulse of Ba^{2+} is again applied to the apical solution.

7. The Overshoot is Characterized by an Increased Permeability of the Tight Junctions

Permeability changes of the paracellular pathway were evaluated in six skins by measuring tracer fluxes of $^{35}SO_4^{2-}$ from the internal to the apical compartment (J^{SO_4}). Overshoots were induced according to Protocol 1 (50 mM KCl on the apical side and a pulse of $BaCL_2$ of 5 mM). The inner solution was Na_2SO_4-Ringer containing tracer sulfate. After a stationary overshoot was reached following Ba^{2+} withdrawal, a recovery period was undertaken by short-circuiting the skins for 60 min with 50 mM KCl plus 5 mM $CaCl_2$ on the apical surface. Then, aiming to return to a condition equal to that preceding the Ba^{2+} pulse, Ca^{2+} was removed and the voltage returned to 40 mV. The sulfate outflux (J^{SO_4}) across the tissue (Fig. 8*A*) follows a time course almost identical to that of G (Fig. 8*B*). During the overshoot phase both J^{SO_4} and G increased significantly in relation to their respective control values measured before the Ba^{2+} pulse. After the end of the Ca^{2+}-induced recovery period, J^{SO_4} and G had returned to levels not significantly different from their respective control pre-Ba^{2+} values. Finally, in the absence of apical Ca^{2+}, J^{SO_4} and G remained constant.

The drop of J^{SO_4} associated to a drop of G observed during the Ba^{2+} pulse (Fig. 8*A*) cannot be

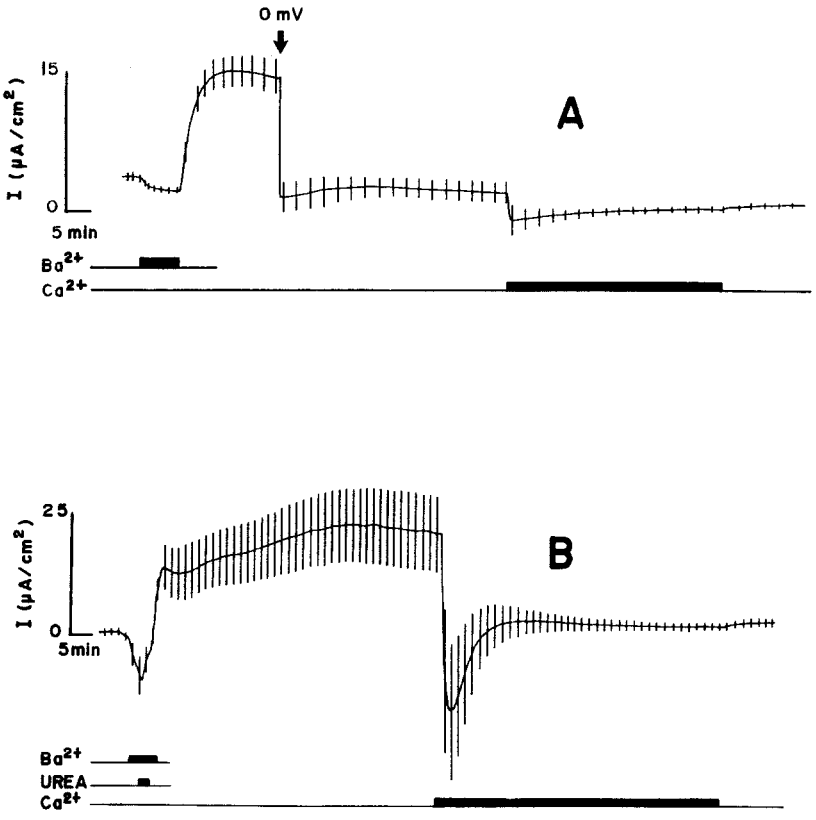

Fig. 6. Representative experiments in frog skins showing a Ca^{2+}-induced recovery of the clamping current (I) and conductance (G) after overshoots of these variables were induced in response to a Ba^{2+} pulse. (A) The overshoot was induced according to Protocol 1 (*see* Materials and Methods) and evolved for 15 min. Thereafter, the skin was short-circuited. After 30 min in this condition, Ca^{2+} (5 mM) was added to the apical solution. A further period of 30 min elapsed and then apical Ca^{2+} was removed. (B) The overshoot was induced according to Protocol 2 (*see* Materials and Methods). After the overshoot had evolved for 60 min, 0.25 mM Ca^{2+} was added to the apical solution for 60 min and then removed. In both panels, G is proportional to the vertical deflections of I.

taken to indicate a reduction of the paracellular permeability in this condition since radioactive SO_4^{2-} could have been trapped as $BaSO_4$ within the epithelium. This ambiguity was avoided by using sucrose as extracellular marker in another group of experiments.

In spite of J^{SO_4} (Fig. 8*A*) increasing during the overshoot phase, the ratio J^{SO_4}/I does not increase when control (0.20 ± 0.017) and overshoot (0.16 ± 0.028) phases are compared. These values indicate that the sulfate current contributes no more than 20% for the total clamping current, the rest of the current being carried mostly by K^+. In addition, we can conclude that the increase of I during the overshoot cannot be ascribed to a selective increase of the sulfate permeability, as the ratio J^{SO_4}/I should increase if this were the case.

In a different group of experiments, fluxes of ^{14}C-sucrose (J^{SUC}) from inner to outer compartments were measured in 11 skins to evaluate the permeability of the paracellular path to a tracer, commonly accepted as a paracellular marker (Smulders & Wright, 1971; Erlij & Martínez-Palomo, 1978; Whittembury et al., 1980), that would not interact with Ba^{2+}. Overshoots were induced according to Protocol 1. Na_2SO_4-Ringer containing ^{14}C-sucrose bathed the inner side of skins. Cold sucrose (1 mM) was present in both compartments. The overshoot phase is characterized by significant increases of J^{SUC} (Fig. 9*A*) as well as of G (Fig. 9*B*), indicating that the TJs became leaky in this condition. When the overshoot was fully developed, $BaCl_2$ 10 mM was readmitted to the apical solution for 15 min and later removed. Readmission of apical Ba^{2+} caused marked and significant reductions of both J^{SUC} (Fig. 9*A*) and G (Fig. 9*B*). When this second skin exposure to Ba^{2+} was terminated, a much larger overshoot took place, with J^{SUC} and G increasing markedly over their previous values. These results unequivocally confirm that the overshoot is associated with an increased permeability of the TJs. In addition, they show that Ba^{2+} added to the apical solution blocks the paracellular route, most probably due to deposition of $BaSO_4$ at the TJ level.

8. K^+ Carries Most of the Current in Both the Control and the Overshoot Phases

The role of K^+ as a current carrier in the control and during the overshoot phases was assessed by replacing K^+ in the apical solution with an equimolar concentration of N-methyl-D-glucamine ($NMDG^+$), a scarcely permeant cation. The skins were submit-

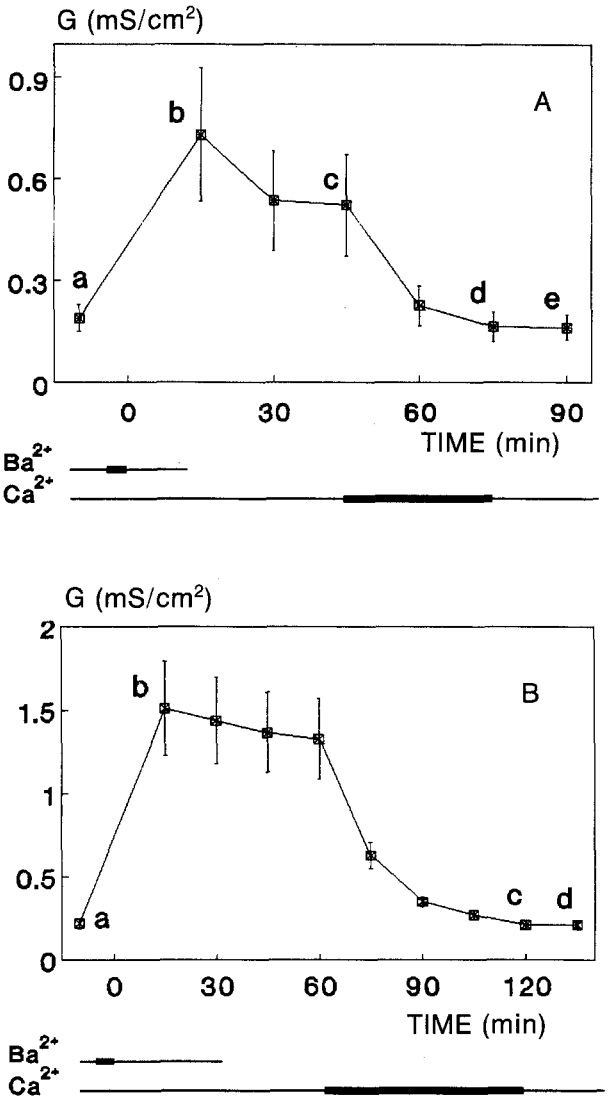

Fig. 7. Increases of conductance (G) caused by apical Ba^{2+} pulses followed by subsequent recoveries induced by apical Ca^{2+}. Time zero corresponds to the end of the Ba^{2+} pulse. Values of G at negative times correspond to control pre-Ba^{2+} measurements. Statistical comparisons were carried out between values indicated by small letters using Student's t-test and Bonferroni's correction. (A) Overshoots were induced according to Protocol 1 (*see* Materials and Methods), following the same scheme of Fig. 6*A*. Except for value b which was obtained at 40 mV, all the other values were measured in the short-circuited condition. Statistical comparisons: a-b: $P < 0.01$; b-c: NS c-d: $P < 0.01$; a-d: NS;d-e: NS ($n = 13$). (B) Overshoots were induced according to Protocol 2 (*see* Materials and Methods), following the same scheme of Fig. 6*B*. Statistical comparisons: a-b: $P < 0.01$; a-c: NS; c-d: NS ($n = 6$).

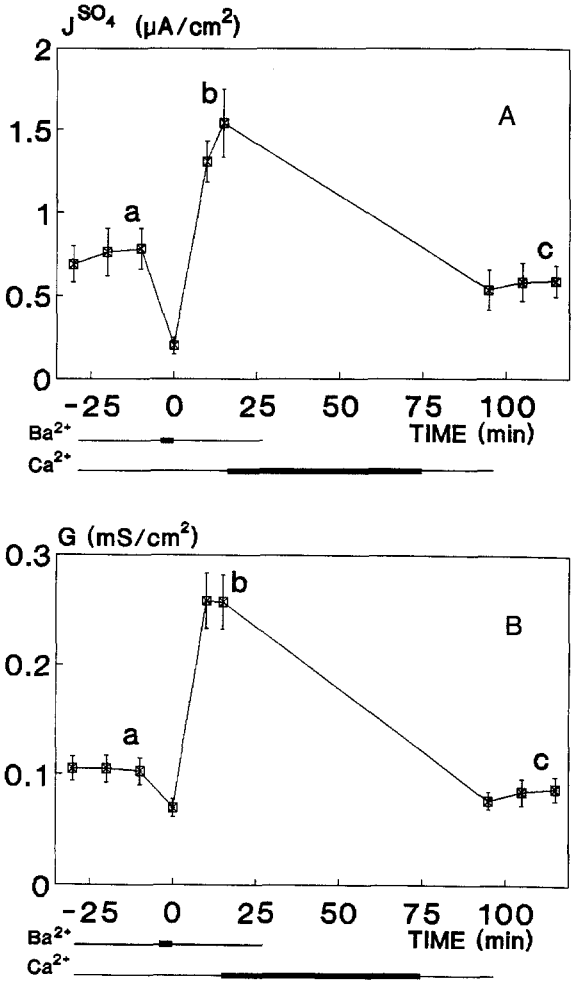

Fig. 8. Increases of sulfate efflux across the skin (J^{SO_4}) and of conductance (G) followed by subsequent recoveries induced by apical Ca^{2+}. Overshoots were induced according to Protocol 1 (50 mM KCl and 5 mM $BaCl_2$, *see* Materials and Methods). After overshoots attained steady state, skins were short-circuited before adding Ca^{2+} (5 mM) to the apical solution. After removal of apical Ca^{2+}, the voltage was returned to 40 mV. Time zero corresponds to the end of the Ba^{2+} pulse. Values at negative times correspond to control pre-Ba^{2+} measurements. Statistical comparisons were carried out between values indicated by small letters using Student's t-test and Bonferroni's correction. (A) Statistical comparisons: a-b: $P < 0.01$; b-c: $P < 0.01$; a-c: NS ($n = 6$). (B) Statistical comparisons: a-b: $P < 0.01$; b-c: $P < 0.01$; a-c: NS ($n = 6$).

ted to Protocol 1. During the control condition before the Ba^{2+} pulse and in the overshoot phase, apical K^+ was temporarily replaced by an equimolar concentration of $NMDG^+$. This ionic substitution caused reduction of both G and I (ΔI and ΔG, respectively), the effect being significantly larger in the overshoot than in the control condition (Table 2). The results permit us to conclude that: (i) K^+ is a major component of the overall conductance, carrying a large fraction of the transepithelial current either in the control and the overshoot phases, and (ii) the transepithelial K^+ permeability increases in the overshoot phase as indicated by ΔI and ΔG being

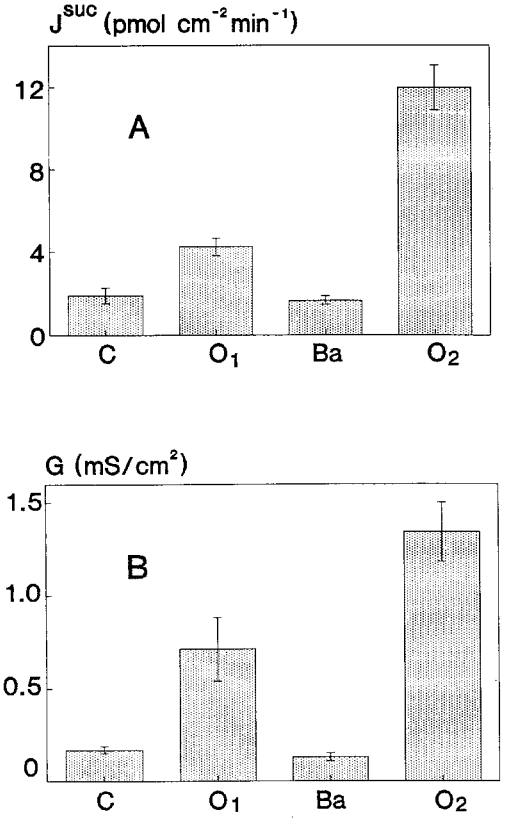

Fig. 9. Effect of apical Ba^{2+} on the sucrose efflux across the skin (J^{SUC}) (*A*) and of conductance *G* (*B*). Overshoots were induced according to Protocol 1 (75 mM KCl and 10 mM $BaCl_2$, *see* Materials and Methods). *C*: Control condition before the Ba^{2+} pulse. O_1: Overshoot steady-state value obtained after an apical Ba^{2+} pulse was applied according to Protocol 1 (*see* Materials and Methods). *Ba*: Value obtained 15 min after Ba^{2+} (10 mM) was readmitted to the apical solution. O_2: Overshoot value attained 15 min after Ba^{2+} was again removed from the apical solution. Statistical comparisons were carried out between values indicated by letters using Student's *t*-test and Bonferroni's correction. (*A*) Statistical comparisons: *C*-O_1: $P < 0.01$; O_1-*Ba*: $P < 0.01$; *Ba*-O_2: $P < 0.01$ ($n = 6$). (*B*) Statistical comparisons; *C*-O_1: $P < 0.01$; O_1-*Ba*: $P < 0.01$; *Ba*-O_2: $P < 0.01$ ($n = 6$).

significantly higher than their control values (Table 2).

9. Overshoots also Occur with Apical Na^+

Experiments were carried out to assess whether overshoots could be elicited with Na^+ in place of apical K^+ (Fig. 10). Two groups of experiments were performed according to Protocols 1 and 2 (*see* Materials and Methods), with the difference that Na^+ equimolarly replaced apical K^+. The contribution of Na^+ for the transcellular conductance and current was avoided by the presence of amiloride (10^{-4} M) in the apical solutions.

These results show that apical K^+ is not needed for the overshoot to occur provided that another cation sufficiently permeant across the open TJs was present in the apical solution.

Discussion

The aim of the present work was to study the effects of a selective deposition of $BaSO_4$ in the TJs of epithelial membranes which led to profound and reversible functional alterations of these structures, as revealed by changes of tissue conductance (*G*), clamping current (*I*), and fluxes of extracellular markers (sulfate (J^{SO_4}) and sucrose (J^{SUC})).

The most striking result was the marked and stable increase of *G* and *I* (overshoot phase) which follows the end of a brief pulse of Ba^{2+} in the apical solution (Results, section 1; Figs. 1 and 2). For the Ba^{2+} pulse to be effective, the inner solution must be a sulfate Ringer and a driving force promoting the meeting of Ba^{2+} and SO_4^{2-} ions within the epithelium must prevail during the pulse (Results, section 2; Fig. 3). As Ba^{2+} and SO_4^{2-} are barely permeable across the cell membranes, and $BaSO_4$ is only slightly soluble (Nancollas & Purdie, 1963), the most likely result of a Ba^{2+} pulse is the selective growth of $BaSO_4$ in the paracellular spaces.

The Ba^{2+} treatment used throughout this study, and the subsequent overshoot phase which develops when apical Ba^{2+} is withdrawn, do not harm the epithelial cells which remain viable after being submitted to such treatments. This conclusion is warranted by (i) the full recovery induced by apical Ca^{2+}, with *G*, *I* and J^{SO_4} returning to values similar to those of the control pre-Ba^{2+} phase (Results section 6; Figs. 6 and 7), (ii) the possibility of inducing a new overshoot after recovery is completed, and (iii) the preservation of skin ability to carry on active Na^+ transport after being submitted to the Ba^{2+} treatment (Results section 5).

The small drop of *G* and *I* observed during the Ba^{2+} pulse (Fig. 1 and Table 1) could result in part from Ba^{2+} blocking apical K^+ channels or cation-selective channels (Ramsay et al., 1976; Granitzer & Nagel, 1990; Van Driessche & Zeiske, 1980, 1985; Van Driessche & De Wolf, 1991) and also from the growth of $BaSO_4$ in the paracellular pathways, blocking these routes. This paracellular effect must certainly be minor as the overall effect of Ba^{2+} on *G* and *I* is also small. In contrast, during the overshoot phase, when Ba^{2+} is tested for a second time, the major falls of *G* and *I* (Fig. 1 and Table 1) are now a strong indication that the newly formed $BaSO_4$ is indeed blocking the paracellular route. A direct support to this notion comes from the experiments

Table 2. Effect of apical $NMDG^+$ for K^+ replacement on the average values of the clamping current (I) and conductance (G) measured in 12 frog skins

Experimental condition	Apical solution					
	K^+	$NMDG^+$		K^+	$NMDG^+$	
	I	I	ΔI	G	G	ΔG
		$\mu A/cm^2$			mS/cm^2	
Control	6.28 ± 0.84	2.93 ± 0.44	3.35 ± 0.54	0.15 ± 0.02	0.10 ± 0.01	0.05 ± 0.01
Overshoot	14.39 ± 1.45	4.65 ± 0.51	9.74 ± 1.16*	0.36 ± 0.04	0.19 ± 0.02	0.17 ± 0.02*

Overshoots were induced according to Protocol 1 (*see* Materials and Methods). ΔI and ΔG are, respectively, the differences between I and G values measured with apical K^+ and apical $NMDG^+$ during both the control pre-Ba^{2+} condition and the overshoot phase. Statistical comparisons: (*) different from value in the control condition ($P < 0.001$), paired t-test.

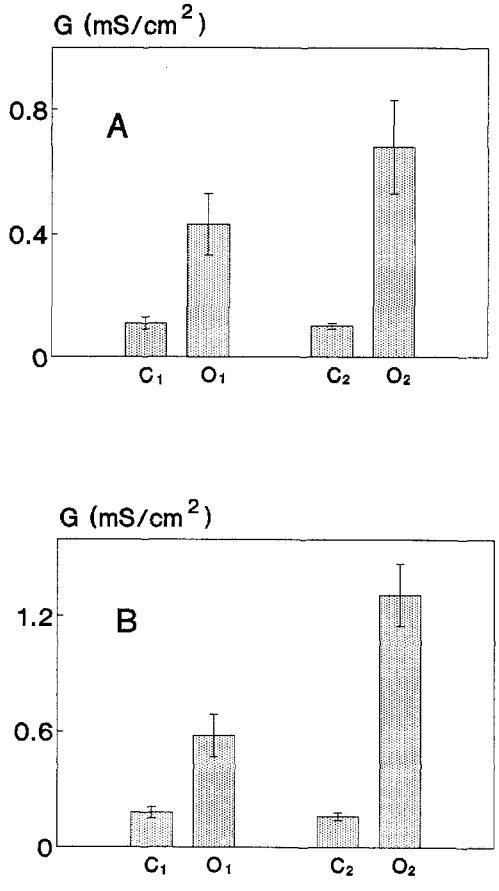

Fig. 10. Average values of the skin electrical conductance (G) measured in the control pre-Ba^{2+} condition (C) and 15 min from the onset of the overshoot (O) in two experimental groups (six skins each). (A) Experiments were performed according to protocols 1 and 2 (*see* Materials and Methods), with the exception that apical K^+ was replaced by an equimolar concentration of Na^+, and amiloride 10^{-4} M was present in the apical solution. Statistical comparisons: O_1-C_1: $P < 0.01$; O_2-C_2: $P < 0.01$ (paired t-test). (B) For the sake of comparison, control experiments were performed according to protocols 1 and 2 with K as the major cation in the apical solution. Statistical comparisons: O_1-C_1: $P < 0.01$; O_2-C_2: $P < 0.01$ (paired t-test).

with sucrose, an extracellular marker, which show a conspicuous reduction of J^{SUC} when a pulse of apical Ba^{2+} was applied during the overshoot (Fig. 9*A*).

The marked facilitation of overshoots by a pulse of urea superimposed to the Ba^{2+} pulse (Results, section 3; Fig. 4) is a strong indication that deposition of $BaSO_4$ occurs in the paracellular pathways, specifically at the TJs, as apical hypertonic urea is known to reversibly open TJs in epithelial membranes (Ussing & Windhager, 1964; Erlij & Martínez-Palomo, 1972; Wade et al., 1973; González et al., 1978). Electron micrographs taken from skins and bladders fixed at the end of the Ba^{2+} pulse (Results, section 4; Fig. 5) corroborate this view, showing the presence of minute amounts of an electron-dense material (presumably $BaSO_4$) in the region of the interspaces where the *zonulae occludentes* are located. The state of increased conductance that characterizes the overshoot phase, on the other hand, has no morphological counterpart, as evaluated by thin-section electron microscopy.

It is a reasonable assumption, on the grounds of results already presented, that minute amounts of $BaSO_4$ do form in the region of the TJs. The junctional proteins could promote a selective nucleation of $BaSO_4$ in the TJ region. Within biological structures, formation of mineral phases is known to be influenced by macromolecules which induce nucleation and orient the pattern of growth (Lowenstam, 1981; Glimcher, 1984; Weiner & Traub, 1984; Williams, 1984; Mann, Sparks & Blakemore, 1987; Wilcock et al., 1988). In addition, as the TJ is a locus of high resistance in the paracellular pathway, it should confine the migration fronts of Ba^{2+} and SO_4^{2-}, contributing to the meeting of these ions at its level.

The overshoot phase, being characterized by a large increase of G, I and the transepithelial fluxes of extracellular markers, J^{SO_4} (Fig. 8*A*) and J^{SUC} (Fig.

9A), necessarily reflects the opening of TJs, as the most important fraction of the paracellular resistance resides in these structures (Martínez-Palomo, Erlij & Bracho, 1971). The mechanism underlying the opening of TJs in response to the Ba^{2+} treatment is not clear at the moment. Opening of TJs could result from the growth of $BaSO_4$ within the TJs during the Ba^{2+} pulse which could deeply alter these junctional elements—a process expected to start and proceed as soon as Ba^{2+} is added to the apical solution. In addition, the presence of $BaSO_4$ should concomitantly block the TJs being disassembled, as already discussed, masking an increase of the paracellular permeability that would otherwise occur. When the Ba^{2+} pulse is terminated, dissolution of the $BaSO_4$ formed within the TJs should start according to the mass action law. The alterations of the TJs induced by the growth of $BaSO_4$ seem to render the TJs leaky when $BaSO_4$ dissolves. The sealing impairment of the TJs could result from (i) a stable association of vestigial amounts of $BaSO_4$ with the TJ proteins, preventing the reassembly, (ii) a defective assembly of the junctional proteins that would not spontaneously return to their original organization upon dissolution of the $BaSO_4$ or, (iii) an endocytotic internalization of TJ elements, a process that could be triggered by the presence of $BaSO_4$ at the TJs. Endocytotic internalization of segments of junctional strands has been described in cultured mammary epithelial cells (Pitelka et al., 1983). A pertinent observation is the impairment of TJ resealing that results from the intromission of lanthanum into the TJs opened by apical hypertonic urea solution (Erlij & Martínez-Palomo, 1972). However, some aspects of that study (Erlij & Martínez-Palomo, 1972) differ from our findings since lanthanum did not lead by itself to TJ opening; its presence did not block the conductance of the paracellular route, and its effect was irreversible in spite of the presence of Ca^{2+} in the apical solution.

Our results indicate that the conductance increase during the overshoot phase occurs without appreciable modifications of the tissue ionic selectivity since: (i) The sulfate current (J^{SO_4}) amounts to about 20% of the total clamping current, both in the control and in the overshoot phases (Results, section 7). (ii) The potassium current (estimated through the substitution of apical K^+ by $NMDG^+$) (Results, section 8) represents at least 50% of the total current (53% in the control and 68% in the overshoot phase (as can be calculated from Table 2). This attests that the TJs are cation selective in the control condition, agreeing with the current opinion (Powell, 1981), and indicating that the same holds in the overshoot phase. These values may be underestimated since the paracellular pathways may be slightly permeable to $NMDG^+$ and the sulfate current is no more than 20% of I. (iii) In all experiments, G, and I are grossly correlated. As apical and basolateral solutions are rather different, this correlation suggests that ionic selectivities are comparable both in the control and in the overshoot phases.

The effect of Ca^{2+} promoting junction sealing (Results, section 6; Figs. 6 and 7) is in agreement with the role of extracellular Ca^{2+} inducing the resealing of TJs previously opened in different experimental conditions (Sedar & Forte, 1964; Cereijido et al., 1978; Meldolesi et al., 1978; Pitelka et al., 1983), and the formation of new TJs (Cereijido et al., 1978; Cereijido et al., 1981; González-Mariscal, Chaves de Ramirez & Cereijido, 1985). An important aspect of the present study is the sidedness of the effect since recovery of G, I and J^{SO_4} to control levels (Results, sections 6 and 7) is induced only when Ca^{2+} is added to the apical solution; the presence of Ca^{2+} in the basolateral solution has no effect.

The sharp drop of I and increase of G which immediately follows the addition of apical Ca^{2+} during an overshoot (Results, section 6; Fig. 6) are strong indications of a direct action of Ca^{2+} on the TJs opened by the effect of $BaSO_4$. This fast response to Ca^{2+} may result from a rapid change in the ionic selectivity of the TJs due to Ca^{2+} screening of negative fixed charges. That no immediate drop of G occurs when Ca^{2+} is added indicates that changes in selectivity occur earlier than the process of TJ sealing itself—sealing which leads to a subsequent slow drop of G toward control pre-Ba^{2+} levels. The changes in selectivity induced by apical Ca^{2+} are features of the TJs made leaky by the deposition of $BaSO_4$, since addition and subsequent removal of apical Ca^{2+} during the control condition (before the Ba^{2+} pulse) (Results, section 6) are without any effect upon G or I.

Our results, despite showing that apical Ca^{2+} interacts with the TJs opened by the $BaSO_4$, do not lead to a conclusion on how apical Ca^{2+} triggers junction sealing, since the effect of apical Ca^{2+} could also result from Ca^{2+} entering the cells via the apical membrane or from the interaction with Ca^{2+} binding sites on the apical aspects of the cells.

The resealing mechanism could result from reassembly of pre-existing junctional elements stemming from TJs disrupted by $BaSO_4$ or from the incorporation of a new junctional component to the membrane, as suggested for MDCK cells in response to the addition of Ca^{2+} to both sides of the monolayer (González-Mariscal et al., 1990).

The present study shows that similar effects of $BaSO_4$ on the TJs can be evoked in the urinary bladder of *R. catesbeiana* and in the skin and urinary

bladder of *B. marinus*, suggesting that the results report general properties of the TJs.

This study incidentally warns about the use of Ba^{2+} as an ion channel blocker in epithelial membranes in association with SO_4^{2-} containing solutions on the contralateral side of the epithelium, as important effects on the paracellular pathways might develop in addition to the desired effects on the transcellular route.

This project was supported by grants from Fundação de Amparo à Pesquisa do Estado de São Paulo (91/0293-7 to F.L.V., and 90/1788-1 to A.S.), and Conselho Nacional de Desenvolvimento Científico e Tecnológico (410068/90-0 and 303633-85/BF to F.L.V.). J.A.C. received a doctoral fellowship from Coordenação de Aperfeiçoamento de Pessoal de Nível Superior/Fundação Universidade do Rio Grande. We thank Dr. Alice T. Ferreira for help in the measurements of free Ca^{2+} concentration.

References

Aboulafia, J., Sanioto, S.M.L., Lacaz-Vieira, F. 1983. Cellular Li^+ opens paracellular path in toad skin: Amiloride blockable effect. *J. Membrane Biol.* **74:**59–65

Balda, M.S., González-Mariscal, L., Contreras, R.G., Macías-Silva, M., Torres-Márquez, M.E., García-Sáinz, J.A., Cereijido, M. 1991. Assembly and sealing of tight junctions: Possible participation of G-proteins, phospholipase C, protein kinase C and calmodulin. *J. Membrane Biol.* **122:**193–202

Benedictis, E.M., Lacaz-Vieira, F. 1982. Electrolytes control flows of water across the apical barrier in toad skin: The hydrosmotic salt effect. *J. Membrane Biol.* **67:**125–135

Bentzel, C.J., Fromm, M., Palant, C.E., Hegel, U. 1987. Protamine alters structure and conductance of *Necturus* gallbladder tight junctions without major electrical effects on the apical cell membrane. *J. Membrane Biol.* **95:**9–20

Bentzel, C.J., Hainau, B., Edelman, A., Anagnostopoulos, T., Benedetti, E.L. 1976. Effect of plant cytokinins on microfilaments and tight junction permeability. *Nature* **264:**666–668

Bentzel, C.J., Hainau, B., Ho, S., Hui, S.W., Edelman, A., Anagnostopoulos, T., Benedetti, E.L. 1980. Cytoplasmic regulation of tight-junction permeability: effect of plant cytokinins. *Am. J. Physiol.* **239:**C75–C89

Cereijido, M., Contreras, R.G., González-Mariscal, L. 1989*a*. Development and alteration of polarity. *Annu. Rev. Physiol.* **51:**785–795

Cereijido, M., González-Mariscal, L., Avila, G., Contreras, R.G. 1988. Tight junctions. *CRC Crit. Rev. Anat. Sci.* **1:**171–192

Cereijido, M., Meza, I., Martínez-Palomo, A. 1981. Occluding junctions in cultured epithelial monolayers. *Am. J. Physiol.* **240:**C96–C102

Cereijido, M., Ponce, A., González-Mariscal, L. 1989b. Tight junctions and apical/basolateral polarity. *J. Membrane Biol.* **110:**1–9

Cereijido, M., Robbins, E.S., Dolan, W.J., Rotunno, C.A., Sabatini, D.D. 1978. Polarized monolayers formed by epithelial cells on a permeable and translucent support. *J. Cell Biol.* **77:**853–880

Chalcroft, J.P., Bullivant, D. 1970. An interpretation of liver cell membrane and junction structure based on observation of freeze-fracture replicas of both sides of the fracture. *J. Cell Biol.* **47:**49–60

Citi, S., Sabanay, H., Jakes, R., Geiger, B., Kendrick-Jones, J. 1988. Cingulin, a new peripheral component of tight junctions. *Nature* **333:**272–276

Claude, P. 1978. Morphological factors influencing transepithelial permeability: A model for the resistance of the *zonula occludens*. *J Membrane Biol.* **39:**219–232

Claude, P., Goodenough, D.A. 1973. Fracture faces of *zonulae occludentes* from "tight" and "leaky" epithelia. *J. Cell Biol.* **58:**390–400

De Wolf, I., Van Driessche, W. 1986. Voltage-dependent Ba^{2+} block of K^+ channels in the apical membrane of frog skin. *Am. J. Physiol.* **251:**C696–C706

Easter, D.W., Wade, J.B., Boyer, J.L. 1983. Structural integrity of hepatocyte tight junctions. *J. Cell Biol.* **96:**745–749

Erlij, D., Martínez-Palomo, A. 1972. Opening of tight junctions in frog skin by hypertonic urea solutions. *J. Membrane Biol.* **9:**229–240

Erlij, D., Martínez-Palomo, A. 1978. Role of tight junctions in epithelial function. *In:* Membrane Transport in biology. G. Giebisch, D.C. Tosteson, H.H. Ussing, editors. pp. 27–53. Springer-Verlag, Berlin

Farquhar, M.G., Palade, G.E. 1965. Cell junctions in amphibian skin. *J. Cell Biol.* **26:**263–291

Fischbarg, J., Whittembury, G. 1978. The effect of external pH on osmotic permeability, ion and fluid transport across isolated frog skin. *J. Physiol.* **275:**403–417

Glimcher, M.J. 1984. Recent studies of the mineral phase in bone and its possible linkage to the organic matrix by protein-bound phosphate bonds. *Philos. Trans. R. Soc. Lond. B.* **304:**479–508

González, Kirchhausen, T., Linares, H., Whittembury, G. 1978. Observations on the action of urea and other substances in opening the paracellular pathway in amphibian skins. *In:* How Organisms Regulate their Internal and External Environment. L. Bolis, S. Maddrell, K. Schmidt-Nielsen, editors. pp. 43–52. Cambridge University, Cambridge

González-Mariscal, L., Chávez de Ramírez, B., Cereijido, M. 1985. Tight junction formation in cultured epithelial cells (MDCK). *J. Membrane Biol.* **86:**113–125

González-Mariscal, L., Contreras, R.G., Bolívar, J.J., Ponce, A., Chávez de Ramírez, B., Cereijido, M. 1990. Role of calcium in tight junction formation between epithelial cells. *Am. J. Physiol.* **259:**C978–C986

Goodenough, D.A., Revel, J.P. 1970. A fine structural analysis of the intercellular junctions in the mouse liver. *J. Cell Biol.* **45:**272–290

Granitzer, M., Nagel, W. 1990. Dual effect of barium on basolateral membrane conductance of frog skin. *Pfluegers Arch.* **417:**207–212

Griepp, E.B., Dolan, W.J., Robbins, E.S., Sabatini, D.D. 1983. Participation of plasma membrane proteins in the formation of tight junctions by cultured epithelial cells. *J. Cell Biol.* **96:**693–702

Grynkiewicz, G., Poenie, M., Tsien, R.Y. 1985. A new generation of Ca^{2+} indicators with greatly improved fluorescence properties. *J. Biol. Chem.* **260:**3440–3450

Gumbiner, B. 1987. Structure, biochemistry, and assembly of epithelial tight junctions. *Am. J. Physiol.* **253:**C749–C758

Gumbiner, B., Simons, K. 1986. A functional assay for proteins involved in establishing an epithelial occluding barrier: Identification of a uvomorulin-like polypeptide. *J. Cell Biol.* **102:**457–468

Hirokawa, N. 1982. The intramembrane structure of tight junctions: an experimental analysis of the single-fibril models using the quick-freeze method. *J. Utrastruct. Res.* **80:**288–301

Kachar, B., Reese, T.S. 1982. Evidence for the lipid nature of tight junction strands. *Nature* **296:**464–466

Kottra, G., Fromter, E. 1990. Barium blocks cell membrane and tight junction conductance in *Necturus* gallbladder epithelium. Experiments with an extended impedance analysis technique. *Pfluegers Arch.* **415:**718–725

Lacaz-Vieira, F. 1986. Sodium flux in the apical membrane of the toad skin: aspects of its regulation and the importance of the ionic strength of the outer solution upon the reversibility of amiloride inhibition. *J. Membrane Biol.* **92:**27–36

Lowenstam, H.A. 1981. Minerals formed by organisms. *Science* **211:**1126–1131

Madara, J.L., Dharmsathaphorn, K. 1985. Occluding junction structure-function relationships in a cultured epithelial monolayer. *J. Cell Biol.* **101:**2124–2133

Mandel, L.J., Curran, P.F. 1972. Response of the frog skin to steady-state voltage clamping. I. The shunt pathway. *J. Gen. Physiol.* **59:**503–518

Mann, S., Sparks, N.H.C., Blakemore, R.P. 1987. Structure, morphology and crystal growth of anisotropic magnetite crystals in magnetotactic bacteria. *Proc. R. Soc. Lond. B* **231:**477–487

Marcial, M.A., Carlson, S.L., Madara, J.L. 1984. Partitioning of paracellular conductance along the ileal crypt-villus axis: A hypothesis based on structural analysis with detailed consideration of tight junction structure-function relationships. *J. Membrane Biol.* **80:**59–70

Martínez-Palomo, A., Erlij, D., Bracho, H. 1971. Localization of permeability barriers in the frog skin epithelium. *J. Cell Biol.* **50:**277–287

Martínez-Palomo, A., Erlij, D. 1975. Structure of tight junctions in epithelia with different permeability. *Proc. Nat. Acad. Sci. USA* **72:**4487–4491

Mazariegos, M.R., Tice, L.W., Hand, A.R. 1984. Alteration of tight junction permeability in the rat parotid gland after isoproterenol stimulation. *J. Cell Biol.* **98:**1865–1877

Meldolesi, J., Castiglioni, G., Parma, R., Nassivera, N., Camilli, P. 1978. Ca^{++}-dependent disassembly and reassembly of occluding junctions in guinea pig pancreatic acinar cells. *J. Cell Biol.* **79:**156–172

Meze, I., Ibarra, G., Sabanero, M., Martínez-Palomo, A., Cereijido, M. 1980. Occluding junctions and cytoskeletal components in a cultured transporting epithelium. *J. Cell Biol.* **87:**746–754

Moreno, J.H. 1974. Blockage of cation permeability across the tight junctions of gallbladder and other leaky epithelia. *Nature* **251:**150–151

Moreno, J.H. 1975. Blockage of gallbladder tight junction cation-selective channels by 2,4,6-triaminopyrimidinium (TAP). *J. Gen. Physiol.* **66:**97–115

Nancollas, G.H., Purdie, N. 1963. Crystallization of barium sulphate in aqueous solution. *Trans. Faraday Soc.* **59:**735–740

Neter, J., Wasserman, W. 1974. Applied Linear Statistical Models. Richard D. Irwin, Homewood. IL

Pinto da Silva, P., Kachar, B. 1982. On tight junction structure. *Cell* **28:**441–450

Pitelka, D.R., Taggart, B.N., Hamamoto, S.T. 1983. Effects of extracellular calcium depletion on membrane topography and occluding junctions of mammary epithelial cells in culture. *J. Cell Biol.* **96:**613–624

Powell, D.W. 1981. Barrier function of epithelia. *Am. J. Physiol.* **241:**G275–G288

Ramsay, A.G., Gallagher, D.L., Shoemaker, R.L., Sachs, G. 1976. Barium inhibition of sodium ion transport in toad bladder. *Biochim. Biophys. Acta* **436:**617–627

Reuss, L., Grady, T.P. 1979. Triaminopyrimidinium (TAP+) blocks luminal membrane K conductance in *Necturus* gallbladder epithelium. *J. Membrane Biol.* **48:**285–298

Reynolds, E.S. 1963. The use of lead citrate at high pH as an electron opaque stain in electron microscopy. *J. Cell Biol.* **17:**208–212

Sedar, A.W., Forte, J.G. 1964. Effects of calcium depletion on the junctional complex between oxyntic cells of gastric glands. *J. Cell Biol.* **22:**173–188

Simons, K. 1990. The epithelial tight junction: Occluding barrier and fence. *In:* Morphoregulatory Molecules. G.M. Edelman, B.A. Cunningham, J.P. Thiery, editors. pp. 341–356. John Wiley & Sons, New York

Simons, K., Fuller, S.D. 1985. Cell surface polarity in epithelia. *Annu. Rev. Cell Biol.* **1:**243–288

Smulders, A.P., Wright, E.M. 1971. The magnitude of nonelectrolyte selectivity in the gallbladder epithelium. *J. Membrane Biol.* **5:**297–318

Stevenson, B.R., Goodenough, D.A. 1984. *Zonulae occludentes* in junctional complex-enriched fractions from mouse liver: Preliminary morphological and biochemical characterization. *J. Cell Biol.* **98:**1209–1221

Stevenson, B.R., Siliciano, J.D., Mooseker, M.S., Goodenough, D.A. 1986. Identification of ZO-1: High molecular weight polypeptide associated with the tight junction (*Zonula occludens*) in a variety of epithelia. *J. Cell Biol.* **103:**755–766

Ussing, H.H. 1971. Introductory remarks. *Philos. Trans. R. Soc. Lond. B* **262:**85–90

Ussing, H.H., Erlij, D., Lassen, U. 1974. Transport pathways in biological membranes. *Annu. Rev. Physiol.* **36:**17–49

Ussing, H.H., Windhager, E.E. 1964. Nature of shunt path and active sodium transport path through frog skin epithelium. *Acta Physiol. Scand.* **61:**484–504

Van Driessche, W., De Wolf, I. 1991. Microelectrode study of voltage-dependent Ba and Cs block of apical K channels in the skin of *Rana temporaria*. *Pfluegers Arch.* **418:**400–407

Van Driessche, W., Zeiske, W. 1980. Ba-induced conductance fluctuations of spontaneously fluctuating K channels in the apical membrane of frog skin (*Rana temporaria*). *J. Membrane Biol.* **56:**31–42

Van Driessche, W., Zeiske, W. 1985. Ionic channels in epithelial cell membranes. *Physiol. Rev.* **65:**833–903

Wade, J.B., Karnovsky, M.J. 1974. Fracture faces of osmotically disrupted *zonulae occludentes*. *J. Cell Biol.* **62:**344–350

Wade, J.B., Revel, J.-P., DiScala, V.A. 1973. Effect of osmotic gradients on intercellular junctions of the toad bladder. *Am. J. Physiol.* **224:**407–415

Weiner, S., Traub, W. 1984. Macromolecules in mollusc shells and their functions in biomineralization. *Philos. Trans. R. Soc. Lond. B* **304:**425–434

Whittembury, G., Martínez, C.V., Linares, H., Paz-Aliaga, A. 1980. Solvent drag of large solutes indicates paracellular water flow in leaky epithelia. *Proc. R. Soc. Lond. B* **211:**63–81

Wilcock, J.R., Perry, C.C., Williams, R.J.P., Mantoura, R.F.C. 1988. Crystallographic and morphological studies of the celestite skeleton of the acantharian species *Phyllostaurus siculus*. *Proc. R. Soc. Lond. B* **233:**393–405

Williams, R.J.P. 1984. An introduction to biominerals and the role of organic molecules in their formation. *Philos. Trans. R. Soc. Lond. B* **304:**411–424